DOI 10.1007/s11141-018-9905-4
Radiophysics and Quantum Electronics, Vol. 61, No. 6, November, 2018
(Russian Original Vol. 61, No. 6, June, 2018)

ANALYSIS OF THE METHODS OF DISCRETE AND SMOOTH FREQUENCY TUNING IN GYROTRONS FOR SPECTROSCOPY, ON THE EXAMPLE OF A GENERATOR OPERATED IN THE 0.20–0.27 THz FREQUENCY RANGE

**N. A. Zavolsky, V. E. Zapevalov, A. S. Zuev,*
O. P. Plankin, A. S. Sedov, and E. S. Semenov**

UDC 621.385.69

We consider the main features of a low-power frequency-tunable gyrotron with an oversized cavity, which is designed for the purposes of nuclear magnetic resonance spectroscopy and other applications and operates in the 0.20–0.27 *frequency range producing an output power of* 200 *W. We study the possibilities of wideband output frequency tuning by exciting a sequence of modes with similar caustics using magnetic-field variations and smooth tuning due to the excitation of modes with a great number of longitudinal variations. Aiming at widening the frequency tuning range, we also analyzed the possibility of smooth frequency tuning determined by controlled variations of the cavity temperature. Specific features of the electron-optical system of such a gyrotron is discussed, along with the possibility of increasing its efficiency by means of single-stage recovery of the residual energy of the electron beam.*

1. INTRODUCTION

Currently, interest in the development of subteraherz and terahertz sources of continuous-wave radiation producing a power of 10–1000 W has greatly increased due to the demands of many practical applications [1, 2]. For some applied problems, the key factor is the possibility to control the radiation frequency, namely, frequency tuning and stabilization [3]. Frequency-tunable radiation sources are used widely, e.g., in nuclear magnetic resonance (NMR) spectroscopy, since sufficiently intense microwaves make it possible to reduce notably the time needed for data accumulation [4, 5]. Additionally, many spectroscopy applications require wideband sources to diagnose many spaced-apart spectral lines. In terms of a set of the parameters required, a promising or even the only type of such a source is the gyrotron [6, 7].

The gyrotron operates at a frequency which is close to the cutoff frequency of an eigenmode of its cavity. The necessary condition of radiation generation in the gyrotron is synchronism of the cavity eigenfrequency ω and one of the cyclotron-frequency harmonics:

$$\omega \approx n\omega_H, \qquad n = 1, 2, 3, \ldots . \tag{1}$$

In this case, the relativistic cyclotron frequency of electrons is determined by the equality

$$\omega_H = \frac{eB}{\gamma m_0}, \tag{2}$$

* alan.zuev@yandex.ru

Institute of Applied Physics of the Russian Academy of Sciences, Nizhny Novgorod, Russia. Translated from Izvestiya Vysshikh Uchebnykh Zavedenii, Radiofizika, Vol. 61, No. 6, pp. 494–504, June 2018. Original article submitted November 20, 2017; accepted June 25, 2018.

where B is the value of the homogeneous longitudinal magnetic field in the interaction space, e is the elementary charge, m_0 is the electron rest mass, and $\gamma = 1 + U$ [kV]/511 is the Lorentz factor. The frequency of the output radiation can be changed by modifying the gyrofrequency, i.e., by changing either the magnetic field, or the accelerating voltage U, while the electrodynamic system should ensure the fulfillment of condition (1).

Wideband frequency tuning in gyrotrons can be realized by means of successive excitation of modes with close caustics by varying the external magnetic field [8, 9]. Up to now, this tuning method has been mainly used in high-power gyrotrons. Passing over from operation of low-power gyrotrons at lower modes with rare spectra to the use of spatially developed modes allows one to realize wideband frequency tuning in such devices, as well. Note that a power of about 1 kW is relatively low for gyrotrons, which determines the specific character of device optimization. This power level is achieved in gyrotrons at relatively low powers of the electron beam, which leads to the necessity of optimization of the cavity profile and the electron-optical system. Along with the above-specified method, gyrotrons provide additional possibilities of frequency tuning by means of exciting longitudinal modes and varying the cavity temperature.

As an example, in what follows we consider a version of a frequency-tunable gyrotron based on a strongly oversized cavity and designed to operate in the 0.20–0.27 THz frequency range producing output radiation up to 200 W in the continuous-wave regime under synchronism with the first gyrofrequency harmonic. This power level is quite sufficient for many applications. The considered gyrotron was developed for operation with the JASTER-10T100 cryomagnet which had a magnetic-field induction of up to 10 T and a borehole diameter of 100 mm [10].

2. CHOICE OF THE GYROTRON PARAMETERS

The size of the borehole of the cryomagnet is the determining factor for choosing the transverse dimensions of the electrodynamic system (i.e., the cavity, the converter, and the output system) and the electron-optical system under the conditions of operating at spatially developed modes. The following operating modes were chosen for realization of stepwise frequency tuning in the above-specified frequency range (the eigenfrequencies of the modes are given in the parentheses): $\mathrm{TE}_{16,6}$ (203.3 GHz), $\mathrm{TE}_{17,6}$ (210.0 GHz), $\mathrm{TE}_{17,7}$ (228.3 GHz), $\mathrm{TE}_{18,7}$ (235.0 GHz), $\mathrm{TE}_{18,8}$ (253.2 GHz), $\mathrm{TE}_{19,8}$ (260.0 GHz), and $\mathrm{TE}_{20,8}$ (266.8 GHz). Preliminary optimization of a multi-frequency gyrotron is usually performed for one of the modes regarded as the main one. As a rule, one of the high-frequency modes is chosen as the main one, since for such modes, all problems become most evident. We chose the $\mathrm{TE}_{19,8}$ mode with a frequency of 260 GHz as the main one. Figure 1 shows the optimal radii R_0 of the beam and frequencies $f = \omega/(2\pi)$ of the specified operating modes for stepwise frequency tuning. The optimal radii R_0 of the electron beam in the working space differ significantly for each mode. Therefore, one should foresee the possibility of changing the overmagnetization coefficient α, which is equal to the ratio of the operating magnetic field to the magnetic field at the cathode ($\alpha = B_0/B_\mathrm{c}$) and determines the radius $R_0 = R_\mathrm{c}/\sqrt{\alpha}$, where R_c is the cathode radius. The chosen cavity profile and the amplitude and phase of the field of the $\mathrm{TE}_{19,8}$ mode are shown in Fig. 2. The coefficient of reradiation in other modes was minimized in the process of optimization of the cavity profile and was equal to less than 0.1 %. Table 1 presents the values of the frequency f, as well as the diffraction and ohmic Q-factors (Q_d and Q_ohm), respectively, for the chosen modes.

The power of the output radiation and the efficiency of the gyrotron are described by the expressions

$$P = \eta_\mathrm{out} IU, \qquad \eta_\mathrm{out} = t_\perp \eta_\perp \eta_\mathrm{c} \eta_\mathrm{w} Q_\mathrm{ohm}/(Q_\mathrm{ohm} + Q_\mathrm{d}), \tag{3}$$

where I and U are the gyrotron beam current and the accelerating voltage, $\eta_\perp$ and η_c are the transverse efficiency and the conversion ratio of the built-in converter, respectively, $t_\perp$ is the ratio of the energy of the oscillatory motion of electrons and the total electron energy, and η_w is the transmission coefficient of the output window. The factor $Q_\mathrm{ohm}/(Q_\mathrm{ohm} + Q_\mathrm{d})$, which determines the decrease in the efficiency due to the ohmic loss, and the optimal radius R_0 for the chosen modes are presented in Table 1. Achieving high efficiency in a low-power gyrotron requires a rather long interaction space, which corresponds to a relatively

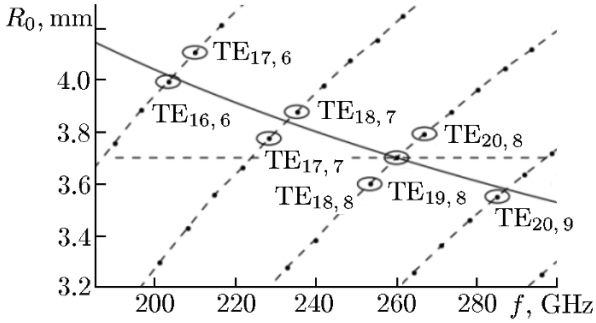

Fig. 1. Optimal radii and frequencies of the operating modes at stepwise frequency tuning. Different radial numbers correspond to the dashed curves, and an individual azimuthal number corresponds to each point. The horizontal dashed line corresponds to the level $R_0 = 3.7$ mm.

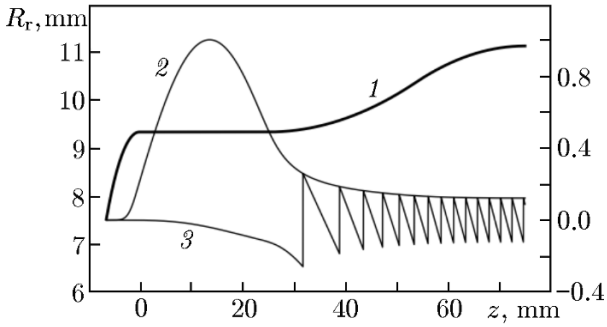

Fig. 2. Cavity profile $R_r(z)$ (curve *1*) and longitudinal distributions of the amplitude and phase (curves *2* and *3*, respectively) in relative units (see the right y axis) of the operating oscillations at the $TE_{19,8}$ mode in the gyrotron.

TABLE 1. Operating parameters of the chosen modes.

Mode	f, GHz	Q_d	Q_{ohm}	$Q_{ohm}/(Q_{ohm}+Q_d)$	R_0, mm
$TE_{16,6}$	203.3	11 310	26 140	0.698	3.995
$TE_{17,6}$	210.0	12 160	26 240	0.683	4.106
$TE_{17,7}$	228.3	14 670	28 320	0.659	3.776
$TE_{18,7}$	235.0	15 660	28 430	0.645	3.879
$TE_{18,8}$	253.2	18 520	30 320	0.621	3.601
$TE_{19.8}$	260.0	19 650	30 430	0.608	3.700
$TE_{20,8}$	266.8	20 820	30 540	0.595	3.786
$TE_{20,9}$	285.0	24 160	32 290	0.572	3.549

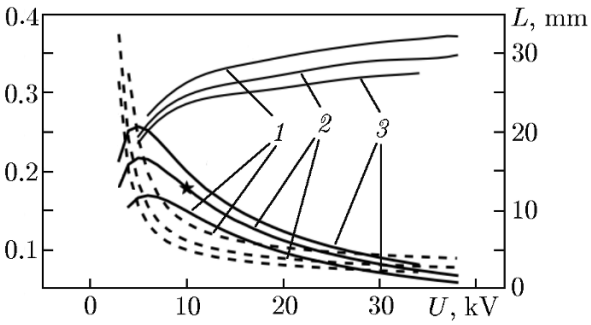

Fig. 3. Efficiency η (thick lines), working current I (dashed lines), and optimal cavity length L (thin lines) as functions of the accelerating voltage U for different pitch factors (lines *1*, *2*, and *3* correspond to $g = 1.0$, 1.2, and 1.4, respectively) at the $TE_{19,8}$ mode for a gyrotron with an output power level of 200 W. The left y axis corresponds to dimensionless values of η and the current I expressed in amperes.

great cavity length, a high diffraction Q-factor and, correspondingly, a large fraction of the ohmic loss (see Eq. (3)).

The electron-wave interaction was optimized preliminarily within the approximation of a fixed longitudinal structure of the high-frequency field [11]. The pitch factor equal to $g = 1.2$ was chosen to ensure stable operation of the gyrotron. Figure 3 presents the efficiency, working current, and optimal length L of the cavity of the gyrotron producing the specified power as functions of the accelerating voltage for various average pitch factors (the pitch factor being the ratio of the average transverse and longitudinal velocities of electrons). From the viewpoint of the device efficiency, the optimal accelerating voltage is equal to 5 kV. However, in this case, developing the system which forms a helical electron beam with the required current level becomes much more complicated. Increasing the voltage up to 10 kV allows one to resolve this issue (see Fig. 3, where the asterisk marks the chosen regime), decreases the sensitivity of the beam parameters to thermal deformations of the electron gun, and reduces the efficiency insignificantly. The relatively low value of the accelerating voltage is chosen to ensure the maximum generation frequency under the condition of a limited value of the magnetic field (see Eqs. (1) and (2)), and, moreover, to make the electric power supply

TABLE 2. Operating parameters of the gyrotron.

Operating modes	$TE_{16,6}$—$TE_{20,8}$
Generation frequency f, GHz	260
Output power P_{out}, W	over 200
Accelerating voltage U, kV	10
Electron beam current I, A	0.13
Electron beam pitch factor g	1.2
Electron beam radius in the working space R_0, mm	3.6–4.1
Cavity radius R_r, mm	8.97
Cavity length L, mm	30
Ohmic loss ratio in the cavity	30.2–40.5 %
Working magnetic field B_0, T	7.3–10.0

and the X-ray protection system simpler and less expensive, which is relevant for a wide range of possible applications of such devices. For each chosen mode in the specified operation regime, the optimal cavity lengths differ insignificantly and range from 24 to 32 mm. On the one hand, according to calculations, increasing the cavity length allows one to excite a greater number of longitudinal waves, which results in widening of the range of continuous frequency tuning. On the other hand, a greater cavity length leads to an increase in the ohmic loss ratio and a decrease in the efficiency. Another relevant factor for the choice of the cavity length is the longitudinal distribution of the magnetic field, whose homogeneous section limits the length of the cavity.

The parameters of the gyrotron operating at the $TE_{16,6}$—$TE_{20,8}$ modes were optimized further within the framework of the theory with the self-consistent longitudinal structure of the high-frequency field [12]. As a result of the optimization, the total efficiency of the gyrotron operating at the above-specified modes was equal to 15.3–18.2% at an electron efficiency of 27.7–33.3%. The main parameters of the multi-frequency gyrotron are presented in Table 2. The calculations were performed with allowance for the relative spread of transverse velocities in the electron beam, which was estimated as 30% [13, 14]. The cyclotron resonance bandwidth $\Delta\omega$ in the gyrotron is determined by the duration T_{pass} of the electron passage through the cavity:

$$\Delta\omega \approx 1/T_{pass} = v_{\|}/L, \tag{4}$$

where $v_{\|}$ is the longitudinal electron velocity. Due to the great length of the cavity, few modes fit in the excitation band, which eliminates the problem of their competition in this gyrotron almost entirely.

The sensitivity of the system to manufacture errors was estimated. The tolerance ΔR_r for variations in the radius of the regular part of the cavity is determined by the deviation of the diffraction Q-factor from the design value by no more than 20%, which corresponds to the following condition [15]:

$$\Delta R_r \leq 0.025 R_r \left(\frac{\lambda}{L}\right)^2, \tag{5}$$

where λ is the operating wavelength, and R_r and L are the radius and length of the regular part of the cavity, respectively. In the process of manufacturing the regular part of the cavity, the condition of a weak variation in the starting current [16] has the form

$$\Delta R_r \leq \frac{2\pi}{16} 10^{-3} R_r \left(\frac{\beta_{\perp 0}^2}{\beta_{\|0}}\right)^3 \frac{L}{\lambda}, \tag{6}$$

where $\beta_{\perp 0}$ and $\beta_{\|0}$ are the initial transverse and longitudinal electron velocities normalized to the velocity of light, respectively. Both estimates yield similar results, namely, that in the manufacture process the radius of the regular part of the cavity cannot deviate from the design value by more than 0.3 μm. The currently available accuracy of manufacturing such cavities is 2.5 μm, while the deviation of the radius of the regular part of the cavity does not exceed 0.2 μm [17], which makes this requirement feasible.

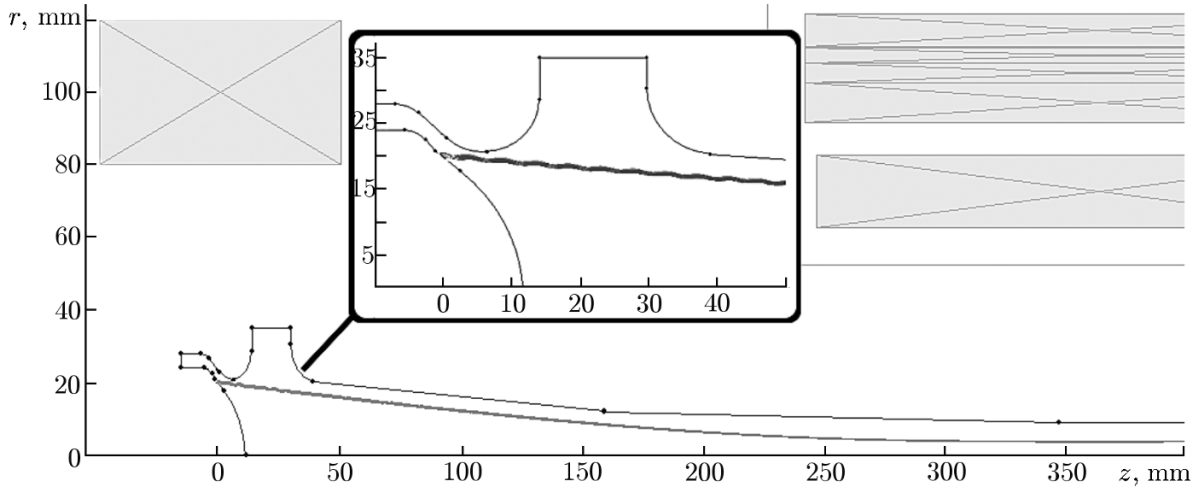

Fig. 4. Drawing of the optimized triode-type magnetron-injection gun.

3. SYSTEM FOR THE ELECTRON BEAM FORMATION

A key element in the gyrotron developments is designing an electron-optical systems producing a helical electron beam with preset parameters. These parameters were preevaluated by means of the adiabatic theory [13], and the follow-up trajectory analysis was performed by using the ANGEL-2DS software code [14]. A triode-type magnetron-injection gun, which made it possible to control adaptively the electron beam parameters due to the possibility of tuning the voltage between the anode and the cathode, was chosen as the electron-optical system, Additional functionality was ensured by a correcting coil installed in the emitter region. It allowed varying the radius of the electron beam in the cavity. For our purposes, a correcting coil with the maximum magnetic-field induction being equal to 0.05 T in the cathode region was sufficient. The drawing of the triode-type electron gun including the shape of the electrodes, the magnetic system, and electron trajectories, is shown in Fig. 4. After preliminary estimations, a cathode 40 mm in diameter was chosen. As the size of the cathode decreases, the sensitivity of the gun to thermal displacements of the cathode and the manufacture accuracy increases. At the same time, it is necessary to increase the electric field at the emitter, which enhances the probability of an electric breakdown. Since the required operating current is rather low, a comparatively narrow emitter is chosen, specifically, its width is equal to 1 mm. Due to a low current density, the spread of electron velocities is determined mainly by the spread of the initial electron velocities, which depends on the emitter properties (surface roughness and initial thermal velocities) and was assumed to be equal to 25% basing on the actual estimations of the above-specified factors. The positional spread of the velocities was less than 2%. The main calculated parameters of the electron-optical system and the produced electron beam are presented in Table 3.

4. TUNING OF THE GENERATION FREQUENCY

Neighboring modes are excited successively in the process of step-wise tuning of the output signal frequency by varying the external magnetic field. The pitch factor of the electron beam can be tuned by adjusting the anode voltage. The chosen modes (shown in Fig. 1) are the closest to the curve, which is obtained within the framework of the adiabatic theory [13] and relates the radius R_0 and the frequency at the other system parameters being fixed (the solid curve in Fig. 1). Table 4 presents the main parameters of these modes. Along with the above-considered modes, one can excite modes with the opposite direction of field rotation with respect to the electron beam ($TE_{-14,7}$, $TE_{-15,7}$, $TE_{-15,8}$, $TE_{-16,8}$, $TE_{-17,9}$, and $TE_{-18,9}$) and the modes interacting with the electron beam at the second maximum of the structural factor ($TE_{12,8}$, $TE_{13,8}$, $TE_{13,9}$, $TE_{14,9}$, $TE_{14,10}$, and $TE_{15,10}$). The eigenfrequencies and optimal radii R_0 of the

TABLE 3. Main parameters of the electron gun.

Cathode radius R_c, mm	20
Distance between the centers of the emitter and the magnet, mm	364.8
Working magnetic field, T	7.3–10
Magnetic field at the cathode, T	0.242–0.358
Magnetic field of the correcting cathode coil, T	0.05
Accelerating voltage U, kV	10
Anode voltage U_a, kV	7.47–9.40
Electric field at the emitter, kV/mm	2.82–3.56
Width of the emitting collar, mm	1
Current density j at the emitter, A/cm^2	0.1
Electron beam current I, A	0.13
Magnetization ratio α	22.56–35.83
Electron beam pitch factor g	1.2
Positional velocity spread	less than 2 %
Total velocity spread	up to 28 %

TABLE 4. Parameters of a step-wise frequency-tunable gyrotron at the beam current $I = 0.13$ and the accelerating voltage $U = 10$ kV.

Mode	f, GHz	P_{out}, W	η_{out}	U_a, kV	B_0, T	δf (at the 10 W level), GHz
$TE_{16,6}$	203.3	237	18.2 %	8.15	7.37	0.17
$TE_{17,6}$	210.0	232	17.9 %	9.20	7.61	0.16
$TE_{17,7}$	228.3	229	17.6 %	7.80	8.27	0.34
$TE_{18,7}$	235.0	222	17.1 %	8.80	8.52	0.33
$TE_{18,8}$	253.2	211	16.2 %	7.50	9.18	0.34
$TE_{19,8}$	260.0	208	16.0 %	8.40	9.42	0.33
$TE_{20,8}$	266.8	199	15.3 %	9.40	9.70	0.33
$TE_{20,9}$	285.0	170	14.1 %	8.20	10.30	0.47

electron beam for these modes are presented in Table 5. Operating at frequencies above 270 GHz requires a cryomagnet with a magnetic field exceeding 10 T (see Table 4). For example, the optimal regime of gyrotron operation at the $TE_{20,9}$ mode requires a field of about 10.3 T. Generation of this mode can be achieved by adding a conventional coil installed between the cryomagnet and the gyrotron body. Replacing a cryomagnet with its off-the-shelf analogs that have the maximum fields of 12 and 13 T allows one to increase the maximum generation frequency proportionally. With no changes required in the gyrotron design for the purpose of increasing the operating frequency, the JASTEC-12T100 cryomagnet can be used, which has a similar longitudinal distribution of the magnetic field.

In the case of excitation of modes with several longitudinal variations of the high-frequency field, negative absorption is observed in two regions of electron transit angles, which correspond to the interaction of the electron beam with a copropagating or counterpropagating wave, whose frequencies are slightly different from the cutoff frequency of the operating mode [18, 19]. The range $\delta\omega$ of such frequency tuning can be estimated by the formula

$$\frac{\delta\omega}{\omega} \approx \frac{1}{8}\left(\frac{\lambda}{L}\right)^2 (q^2 - 1), \tag{7}$$

where q is the longitudinal index of the operating mode in the cavity. The number of the longitudinal modes excited by a smooth variation in the magnetic field, depends mainly on the working current and the ratio λ/L of the operating wavelength to the cavity length. Thus, according to the calculations within the framework of the self-consistent model [12], the $TE_{16,6}$ and $TE_{17,6}$ modes can be excited in the chosen regime of gyrotron

TABLE 5. Parameters of the modes with opposite directions of the field rotation with respect to the electron beam and the modes, which interact with the electron beam at the second maximum of the structural factor and can be used for wideband frequency tuning.

Mode	f, GHz	R_0, mm
$TE_{-14,7}$	207.9	3.91
$TE_{-15,7}$	214.7	4.01
$TE_{-15,8}$	232.6	3.71
$TE_{-16,8}$	239.5	3.81
$TE_{-17,9}$	264.2	3.64
$TE_{-18,9}$	271.1	3.73
$TE_{12,8}$	211.7	3.97
$TE_{13,8}$	218.7	4.10
$TE_{13,9}$	236.2	3.79
$TE_{14,9}$	243.3	3.90
$TE_{14,10}$	260.8	3.64
$TE_{15,10}$	267.9	3.74

operation with only one or two longitudinal variations. During operation at the $TE_{17,7}$, $TE_{18,7}$, $TE_{18,8}$, $TE_{19,8}$, and $TE_{20,8}$ modes, generation of modes with three longitudinal variations is possible. The range $\delta f = \delta\omega/(2\pi)$ of continuous tuning for such modes at a level of 10 W is presented in Table 4. Estimating the frequency tuning by formula (7) yields slightly overstated results as compared with those obtained within the framework of the self-consistent model.

In low-power gyrotrons, additional adjustment of the frequency can be realized by varying the cavity temperature (by about 3–4 MHz/°C). By changing the liquid-coolant temperature by 25°, one can adjust the frequency of the radiation by up to 0.1 GHz. This frequency adjustment method allows one to extend the continuous tuning range to 0.27 GHz for the $TE_{16,6}$ and $TE_{17,6}$ modes and to 0,44 GHz for the $TE_{17,7}$, $TE_{18,7}$, $TE_{18,8}$, $TE_{19,8}$, and $TE_{20,8}$ modes. This method was already used successfully earlier in the low-power gyrotrons developed for spectroscopy applications [19, 20]. A necessary precondition of realizing this method in practice is the structural possibility of extending the gyrotron cavity and a separate cooling contour freely, thus ensuring control over the temperature of the cooling liquid.

Multimode continuous frequency tuning in such a gyrotron is impossible because of the low operating current, which hampers the excitation of modes with several longitudinal variations. Additionally, wideband continuous tuning is complicated by the large length of the cavity, which exceeds only slightly the minimum length at which generation at all selected modes.

5. ELECTRON BEAM COLLECTOR

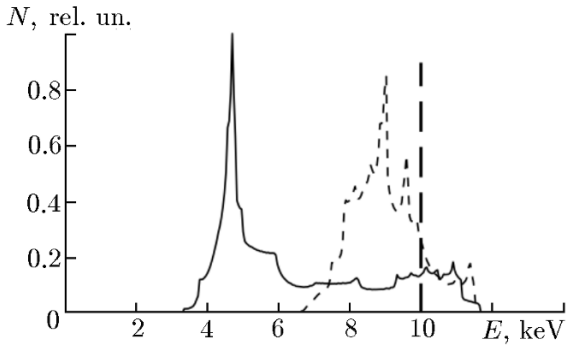

Fig. 5. The energy spectrum $N(E)$ of the spent electron beam for the $TE_{20,8}$ mode with one longitudinal variation (solid line) and for the mode with two longitudinal variations (dashed line). The initial energy of the electron beam corresponds to $E_0 = 10$ keV.

The electron beam collector system is not a serious design issue at the planned levels of the gyrotron output power. A cylindrical collector 70 mm in diameter is proposed for the considered gyrotron. The average thermal load on it is equal to 28 W/cm^2 (with a peak load of 57 W/cm^2), which makes it possible to avoid forced water cooling.

Since, when electrons interact with the high-frequency field in the cavity, they loose not more than a certain fraction of their energy, one can increase the gyrotron efficiency by extracting the residual energy of the spent electron beam after it exits from the interaction space (recovery) [21–32]. In the case of single-stage electron beam recovery, the final efficiency is determined by the following well-known formula (see, e.g., [23]):

$$\eta = \frac{W}{W - W_{\min}}\eta_{\text{out}}, \tag{8}$$

where W is the total electron energy, and $W_{\min}$ is the minimum energy of the particles in the spent beam. In the case of modes with one longitudinal variation, the minimum energy of the spent electron beam is equal to 32% of the initial electron energy (see Fig. 5). Due to a potential difference of 3 kV between the collector and the cavity, the process of single-stage recovery of the electron beam increases the total efficiency from

15.2–18.2% to 21.7–26.0%. In the case of operation at modes with two longitudinal variations, recovery of the energy of the spent electron beam allows increasing the total efficiency from 2.2–3.7% to 5.50–9.35% for the $TE_{20,8}$—$TE_{16,6}$ modes, respectively. Along with the higher efficiency and the possibility to use lower-power supply units, the gyrotrons with recovery reduce coolant consumption and decrease the levels of X-ray radiation from the collector.

6. RADIATION OUTPUT SYSTEM

When designing gyrotrons, one has to solve the problem of converting the operating mode and outputting the radiation. On interacting with the electron beam, the operating mode, which has a complex transverse structure, is transformed into a Gaussian wave beam in a system of quasioptical mirrors and output through the output window. There are methods of constructing highly efficient multimode converters, in which the diffraction loss is less than 5% of the radiation energy [24], including the variant for modes with different rotation directions [25].

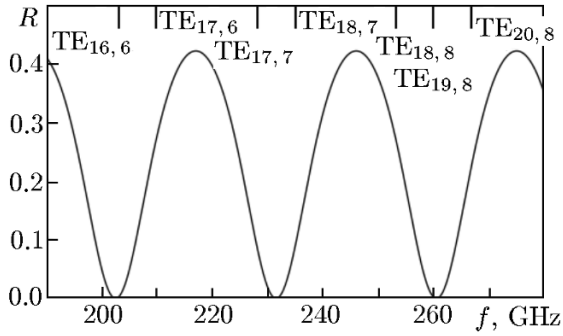

Fig. 6. Dependence of the reflection coefficient on the radiation frequency for a single-disk window. The thickness of the output window is optimized for seven modes.

The material frequently used for output windows in low- and medium-power gyrotrons is boron nitride (BN), since it is considerably cheaper than other materials, and a great experience of working with it has been already accumulated [26]. The required transmission level for some frequencies is available, when a single disk is used, but the bandwidth of such a window is insufficient to cover the entire 0.20–0.27 THz range. The thickness of the single-disk output window, which was optimized for seven modes (see Table 4) for the perpendicular incidence of the transverse electric wave, was equal to 2.38 mm (see Fig. 6) with the greatest reflection coefficient being 27% for the $TE_{18,8}$ mode. Although in some cases the lesser thickness leads to a decrease in the reflection coefficients for the specified modes, it cannot be ensured due to the pressure difference at the window walls. Transmission coefficients can be increased significantly by using windows with greater thicknesses, but such BN windows are not manufactured commercially. Therefore, one can use a leucosapphire window having a thickness of 7.71 mm, for which the greatest reflection coefficient among the seven chosen modes is equal to 12.6%. Another way to achieve a low value of the reflection coefficient is to add an antireflection plate. A low thermal load on the output window allows one to replace the antireflection plate in the operation process in the case of transition to another operating mode, thus reducing the reflection coefficient for each mode significantly. In the case of the incidence of transverse magnetic waves, the most promising method is the use of the Brewster window. Additional possibilities of minimizing the reflection coefficient are provided by the use of a double-disk window or a wideband profiled window [27].

7. CONCLUSIONS

We have analyzed the possibility of discrete and smooth tuning of the operating frequency in a multifrequency subterahertz gyrotron producing an output power of about 200 W. The resulting efficiency for the chosen parameters of the beam and the electrodynamic system with allowance for single-stage recovery is 21.7–26.0% for the $TE_{20,8}$—$TE_{16,6}$ modes, respectively. Efficiency limitation is determined mainly by the high ohmic loss in the gyrotron cavity. In the case of modes with two longitudinal variations, recovery of the energy of the spent electron beam allows increasing the total efficiency by more than two times, up to 5.50–9.35% depending on the operating mode. By varying the external magnetic field (and adjusting the anode voltage, whenever necessary), one can ensure selective excitation of various modes, thus achieving wideband discrete frequency tuning in the range 0.20–0.27 THz. Depending on the operating mode, it is possible to achieve continuous frequency adjustment from 0.27 to 0.44 GHz by exciting modes with several

longitudinal variations of the high-frequency field and using additional frequency adjustments by controlling the cavity temperature.

The authors are grateful to M. Yu. Glyavin and V. N. Manuilov for interest in this work and constructive comments. The work was supported by the Russian Foundation for Basic Research (project No. 15-42-02380 r_povolzhye_a).

REFERENCES

1. M. Yu. Glyavin, G. G. Denisov, V. E. Zapevalov, et al., *Phys. Usp.*, **59**, No. 6, 595 (2016).
2. N. Kumar, U. Singh, T. P. Singh, and A. K. Sinha, *J. Fusion Energy*, **30**, No. 4, 257 (2011).
3. J. H. Booske, R. J. Dobbs, C. D. Joye, et al., *IEEE Trans. Electron Devices*, **1**, No. 1, 54 (2011).
4. L. R. Becerra, G. J. Gerfen, R. J. Temkin, et al., *Phys. Rev. Lett.*, **71**, No. 21, 3561 (1993).
5. V. S. Bajaj, C. T. Farrar, M. K. Hornstein, et al., *J. Magnetic Res.*, **160**, 85 (2003).
6. G. S. Nusinovich, M. K. A. Thumm, and M. I. Petelin, *J. Infrared, Millimeter, Terahertz Waves*, **35**, No. 4, 325 (2017).
7. T. Idehara and S. P. Sabchevski, *J. Infrared, Millimeter, Terahertz Waves*, **33**, No. 7, 667 (2012).
8. M. Thumm, A. Arnold, E. Borie, et al., *Fusion Eng. Design*, **53**, 407 (2001).
9. V. E. Zapevalov, A. A. Bogdashov, G. G. Denisov, et al., *Radiophys. Quantum Electron.*, **47**, Nos. 5–6, 395 (2004).
10. M. Yu. Glyavin, A. V. Chirkov, G. G. Denisov, et al., *Rev. Sci. Instr.*, **86**, No. 5, 054705 (2015).
11. G. S. Nusinovich and R. É. Érm, *Elektron. Tekhn., Ser. I, Electron. SVCh*, 8, 55 (1972).
12. N. A. Zavolsky, V. E. Zapevalov, and M. A. Moiseev, *Radiophys. Quantum Electron.*, **44**, No. 4, 318 (2001).
13. Sh. E. Tsimring, *Electron Beams and Microwave Vacuum Electronics*, Wiley-Interscience (2006).
14. O. P. Plankin and E. S. Semenov, *Nizhny Novgorod Univ. Bull. Ser. Fizika*, **8**, 2, 44 (2013).
15. V. E. Zapevalov and O. V. Malygin, *Izv. Vyssh. Uchebn. Zaved., Radiofiz.*, **26**, No. 7, 903 (1983).
16. G. S. Nusinovich, R. Pu, O. V. Sinitsyn, et al., *IEEE Trans. Plasma Sci.*, **38**, No. 6, 1200 (2010).
17. A. C. Torrezan, M. A. Shapiro, J. R. Sirigiri, et al., *IEEE Trans. Electron Devices*, **58**, No. 8, 2777 (2011).
18. M. K. Hornstein, V. S. Bajaj, R. G. Griffin, et al., *IEEE Trans. Electron Devices*, **52**, No. 5, 798 (2005).
19. M. Yu. Glyavin, G. G. Denisov, V. E. Zapevalov, et al., *Radiophys. Quantum Electron.*, **58**, No. 9, 649 (2016).
20. N. P. Venediktov, V. V. Dubrov, V. E. Zapevalov, et al., *Radiophys. Quantum Electron.*, **53**, No. 4, 237 (2010).
21. A. Sh. Fix, V. A. Flyagin, A. L. Goldenberg, et al., *Int. J. Electron.*, **57**, No. 6, 821 (1984).
22. K. Sakamoto, M. Tsuneoka, A. Kasugai, et al., *Phys. Rev. Lett.*, **73**, No. 26, 3532 (1994).
23. M. Yu. Glyavin, A. N. Kuftin, N. P. Venediktov, and V. E. Zapevalov, *Int. J. Infrared Millimeter Waves*, **18**, No. 11, 2129 (1997).
24. A. V. Chirkov, G. G. Denisov, A. N. Kuftin, et al., *Tech. Phys. Lett.*, **33**, No. 4, 350 (2007).
25. A. V. Chirkov, G. G. Denisov, A. N. Kuftin, *Appl. Phys. Lett.*, **106**, No. 26, 263501 (2015).
26. V. V. Parshin, *Int. J. Infrared Millimeter Waves*, **15**, No. 2, 339 (1994).
27. S. N. Vlasov and E. V. Koposova, *Radiophys. Quantum Electron.*, **52**, No. 10, 782 (2009).